Contents lists available at *Dergipark*

Journal of Scientific Reports-A

journal homepage: *https://dergipark.org.tr/tr/pub/jsr-a*



E-ISSN: 2687-6167 ***Number 65, June 2026***

RESEARCH ARTICLE

Receive Date: 28.10.2025 *Accepted Date: 07.01.2026*

DFT study: investigation of electronic properties and bond behavior of graphene structure doped with various boron clusters

Hilal Küçük[a,*], İsa Baruğ[b], Meryem Yurt[c]

[a,*]*Gazi University, Faculty of Science, Ankara-Türkiye, ORCID Number: 0000-0002-6655-5602*
[b]*Gazi University, Faculty of Science, Ankara-Türkiye, ORCID Number: 0009-0005-6830-3248*
[c]*Gazi University, Faculty of Science, Ankara-Türkiye, ORCID Number: 0009-0009-6589-1768*

Abstract

2d materials occupy a very important place, especially in industrial areas. Graphene is used in many areas through its stable structure, high durability and special electronic structure. The graphene surface is modified by various methods in order to increase the efficiency of the structure according to the working area and to obtain more stable structures in different conditions. In this study, the electronic properties of the doped various boron clusters on graphene were examined using a computational program-DFT and stable structures were observed. The primary reason for choosing boron atoms as the atom to be doped is that the boron atom is as light as carbon. Among the boron cluster, B_N ($9 \geq N \geq 3$), the most stable structures are B_5 and B_6 cluster structures. Only the B_3-Gr structure graphene can stand horizontally on the surface. To understand bond type of atoms, the bond properties are calculated with Crystal orbital Hamiltonian population analysis. The vast majority of structures show semiconductor properties while B_3-Gr Configuration and B_6-Gr structure.
© 2023 DPU All rights reserved.
Keywords: Graphene; doping; boron; electronic properties; bond structure; dft;

1. Introduction

The astronomical surface area-to-mass ratio of single-layer materials indicates that they can serve as highly efficient functional materials. Because of the large surface area on which ions can interact, two-dimensional materials can be used as batteries and enables tunable electronic behavior relevant to 2d devices for researchers in optics and photonics, chemistry, applied physics, and many other disciplines [1]. The examples for monolayer materials are given borophene [2], germanene [3], silicone and stanine [3], SnO [4], etc..

Küçük, H., Baruğ, I. & Yurt, M. (2026) / Journal of Scientific Reports-A, 065, 17-28
*Corresponding Author: Hilal Küçük, Tel: 00903122021325, *E-mail address:* hilalkucuk@gazi.edu.tr

Among single-layer materials, graphene is the most extensively investigated. It is formed by covalent bonding between carbon atoms in the hexagonal honeycomb-shaped lattice structure [5]. Graphene possesses characteristic structural and electronic features, good electrical and thermal conductive property, efficient tunneling by overcoming potential obstacles, mechanical durability and flexibility [6].

Graphene is employed in conductive inks [7], wearable technology [8], sensors [9-11], coatings [12, 13], battery technologies [14], supercapacitors [15], transistors [16], catalyzer [17] etc.. Under normal conditions, pure graphene is not chemically active and also has a zero band gap. Therefore, this intrinsically restricts its applicability in electronic devices. However, the physical and chemical properties of graphene can be changed by adding different atoms or clusters of atoms to graphene, and the fields of its study can be expanded [18, 19]. A widely explored strategy involves the incorporation of transition metals[20, 21]. Xin et al. [22], tested the monatomic 3d transition metals (TM=Ti, V, Cr, Mn, Fe, Co, Ni and Cu) doped on the surface of N4 embedded graphene (Gr) with different concentration. Its electronic and magnetic properties are adjusted by changing the transition metal atoms. Also, there is a direct relationship between the performance of the surface and doped atom concentration. C. Jin et al. [23] focused graphene (Gr) and N embedded graphene (N-Gr) surface with doping transition metals clusters(n is number of cluster, n = 1–4).The 3d metal clusters showed identical geometries on the Gr and N-Gr surfaces, and the clusters adsorbed on the N-Gr surface had significantly stronger interaction than those on the pristine Gr surface. Instead of adding metals to grafene surface, non-metal dopants (N, O, B, etc.) can be performed on the graphene surface because they are cheaper and much lighter. P. Raji and V. Jindal [24] represent that the electronic properties of graphene transfers from semi-metal to semiconductor when doping boron and nitrogen atoms to graphene. The addition of boron and nitrogen atoms do not increase the band gap very much, but only increase it to ~0.14 eV. In the other investigation [25], graphene oxide nanoribbons is doped by oxygen atoms. The modified material measurably semiconducts by changing the band gap in the range of 1.151–1.317 eV. Boron, one of the light metals, has various uses such as heat-resistant glass and internal combustion engine pistons, and the surface coating industry. In addition, boron is used in the field of health (in the treatment of brain cancer, as a sterilization material in eye inflammations, in the production of ointments, neuroprotective effect in Alzheimer's and Parkinson's diseases, etc.), heat-abrasion resistant fiber optic cables, dielectric materials, semiconductor materials, capacitors, batteries [26-29]. Boric element borax decahydrate can be used in energy storage, neutron scavengers in nuclear applications, boric acid and borates as combustion inhibitors, perborate in cleaning and bleaching, sodium boron hydrate in waste cleaning, and sodium tetra borate as fuel additive [30-32]. One of the important researches for boron structures was carried out by L. Li et al. [33] It was determined that boron clusters were generally stable in planar (2d) structures. In addition, when adding metals to boron clusters, boron can increase the structural diversity and flexibility of structures and adjust the catalytic, magnetic and optical properties of these materials. Another study on boron clusters was conducted by D. Kang et al. [34] They obtained beryllium-doped boron clusters and provided that these clusters show significant similarities with borophene, and show metallic and high conductivity properties. It is aimed that the BeB16 cluster can be used to develop 2d materials by acting as a metallo-borophenous material. A. Kochaev et al. [35] investigated the electronic structures of graphene and boron surfaces. A covalent combination of periodically hollow borophene and graphenylene was tested and the resulting hetero borophene-graphene is found to be a narrow-pitch semiconductor. In this study, we tackle the constraint of pure graphene by methodically examining its alteration with boron clusters of varying dimensions (B_3–B_9) by DFT. While previous studies have focused on single-atom non-metal doping or transition-metal functionalization, the effect of boron clusters on the electronic properties of graphene remains largely unexplored. By analyzing the stability, charge transfer, band structures, and density of states of boron-cluster–doped graphene using Density Functional Theory (DFT), this work provides new insights into how cluster size influences the transition between semi-metallic and semiconducting behavior. These findings not only fill a gap in the theoretical understanding of graphene functionalization but also highlight boron-cluster–doped graphene as a promising candidate for lightweight, tunable materials in future nanoelectronic and sensor applications.

2. Materials and methods

All data are calculated using the Density Functional Theory based Quantum Espresso simulation program. Grimme (DFT-D3),dispersion correction is used for weak interactions in all calculations [36]. The projector augmented wave method (PAW) is used to identify interactions between valence and nuclei [37-39]. The cut energy for the plane wave is taken as 60 Ry, the cut energy is taken as 660 Ry for the electronic charge density. Graphene is composed of 5x5x1 supercells and has 50 atoms. 4x4x1 Mokhorst-Pack k-point sets are selected. The boron clusters used in the study are shown in Fig. 1. Wan-Lu et al. [33] have shown that many boron clusters have a two-dimensional structure

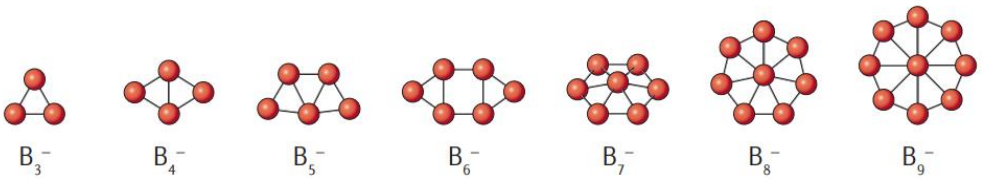


Fig. 1. Boron clusters[33].

Table 1 represents the average bond lengths of the boron clusters, and the bond lengths and height of optimized boron cluster-doped graphene (B-Gr) structures are given in
Table 2. Formation energy ($\boldsymbol{E_f}$) is,

$$E_f = E_{Gr+B} - E_{gr} - E_B \quad (1)$$

when $\boldsymbol{E_{Gr+B}}$ is the total energy of the structure of B-Gr, $\boldsymbol{E_{Gr}}$ and $\boldsymbol{E_B}$ the total energy of the graphene surface and pure boron clusters, respectively. If the formation energy value is negative, the surface is formed with an exothermic process. An increase in the magnitude of the formation energy indicates that the structure is more stable. Moreover, chemical bond information is looked at to learn more about how stable the material is. One method of collecting chemical bonding data that describes the nature of bonding in layers and adsorbed configurations is Crystal orbital Hamiltonian population (COHP) [40]. The electronic wave functions are employed to produce bonding data through COHP calculation, which made by Lobster code [41, 42]. In COHP calculation, Integrated Crystal Orbital Hamilton populations (ICOHP) analyses give direct measurement of the strength of interatomic bonds (covalent bond strength). Greater negative results for ICOHP indicate a stronger covalent bond. If ICOHP values are close to zero, ionic character is more dominant. The result of ICOHP is evaluated by summing spin-up and spin-down values. Calculations of Bader charge is [43]

$$\Delta q = q_\alpha - q_\beta \quad (2)$$

when $\mathbf{q_\alpha}$ is the total charge of the boron atoms in $\mathbf{B_N}$-Gr structure and $\mathbf{q_\beta}$ is the total charge of the optimized boron clusters alone. Bader is used for the analysis of charge distribution between atoms in the obtained structures.

3. Results and discussion

In a theoretical study by Ihsan Boustani, boron clusters were examined [44]. In Table 1, the average bond lengths (d_o) between borons, and the average of bond lengths (d_b) in Ihsan Boustani's study are compatible with their study.

Table 1: The average B-B bond lengths (d_o) in boron clusters and the mean B-B bond lengths (d_b) values in Ihsan Boustani's study [44].

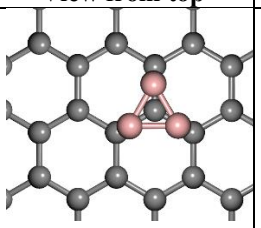
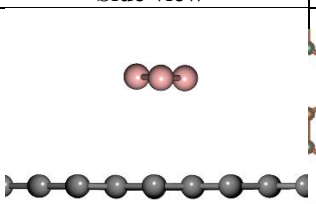
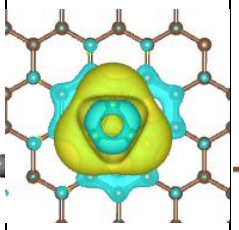
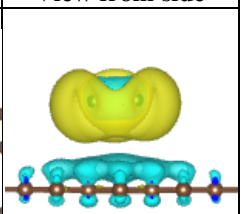
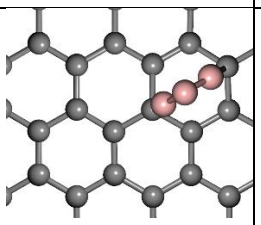
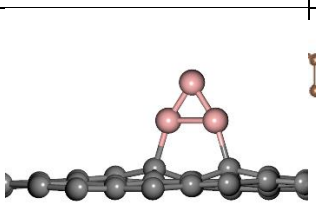
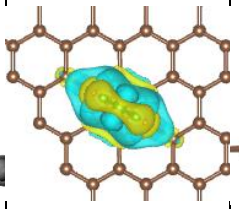
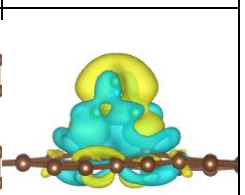
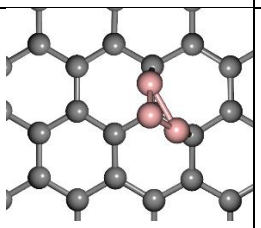
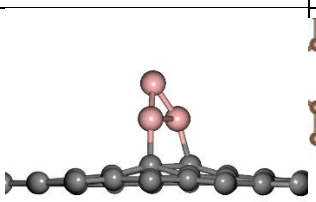
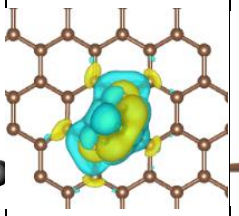
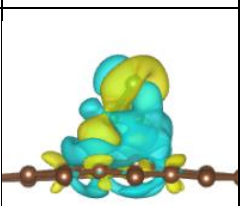
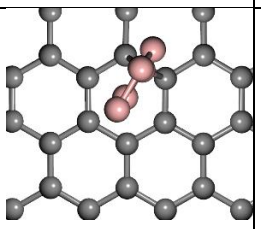
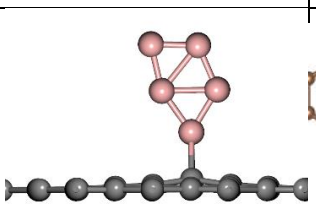
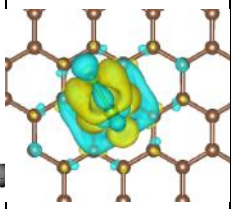
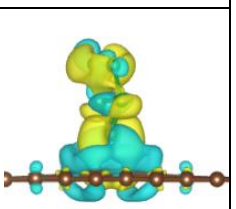
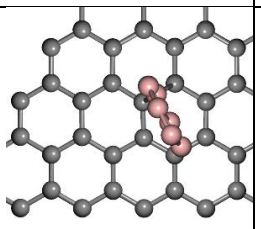
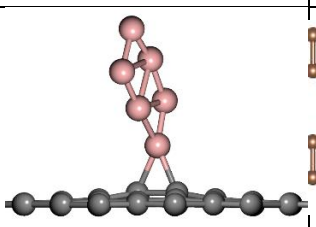
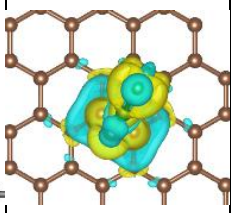
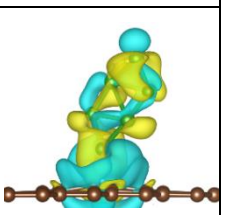
Clusters	d_o (Å)	d_b (Å)
B_3	1.554	1.553
B_5	1.65	1.57
B_6	1.575	1.561
B_7	1.639	1.655
B_9	1.76	1.75

All boron structures are placed on the surface as "hollow site" (middle of the hexagonal cavity), "bridge site" (between two carbon atoms), "top site" (on top of a carbon atom). Although the clusters with more boron atoms are doped horizontally, they stabilize vertically after optimization as seen in Fig. 2. B5-Gr and B6-Gr structures are the most stable structures.

Table 2. Optimized B-Gr structures, B-Gr height (h), B-B bond length (di) between boron cluster atoms, formation energy (Ef) and bader charge (Δq) values. The lowest and highest distances are added in d_i.

Structure	h (Å)	d_i (Å)	E_f (eV)	Δq (q)	Band gap (eV)
B_3-Gr configuration 1	3.53	1.55	-0.45	0.29	0.43
B_3-Gr configuration 2	1.65	1.52-1.77	-1.06	-0.73	0.65
B_3-Gr configuration 3	1.54	1.52-1.75	-1.058	-0.98	0.0
B_5-Gr	1.52	1.53-1.88	-1.52	-0.399	0.17
B_6-Gr	1.70	1.52- 1.85	-1.87	-0.37	0.0
B_7-Gr	1.79	1.58- 1.77	-1.00	-0.14	0.215
B_9-Gr	1.79	1.55- 2	-1.20	-0.05	0.15

Comparing to Table 1, the bond length (d_i) between two boron atoms interacted with carbons are stretched as seen in Table 2. The bond distance between atoms far from the surface becomes at the level of 1.5 Å. The horizontal position of cluster **B_3** to the graphene surface in Fig. 2 has the lowest formation energy with -0.45 eV, it has the least strongly bound with graphene compared to the others. Also, the **B_3** cluster is vertically located both in the middle of the carbon honeycomb (configuration 2) and between the two carbons (configuration 3), but the formation energies are similar. Since there is no strong bonding between the horizontal **B_3** cluster (configuration 1) and graphene, the B-B bond lengths are almost unchanged in the **B_3-Gr** structure. However, on the other stable structures (configuration 2 and 3) (**$|E_f| > 1$ eV**), more changes are observed because of the stronger interaction between graphene and the boron cluster. Generally, the more stable structure has the more changes. The height of the cluster to the graphene surface has decreased due to the strong interaction between the graphene and boron cluster in stable structures of **B_3-Gr**. Although the clusters with more boron atoms are doped horizontally, they stabilize vertically after optimization as seen in Fig. 2. **B_5-Gr** and **B_6-Gr** structures are the most stable structures. Although it cannot establish a complete relationship between the formation energy and the height from the surface, the B-B bonds interacting with the surface are more extended.

Structure	View from top	Side view	View from top	View from side
B_3-Gr configuration 1				
B_3-Gr configuration 2				
B_3-Gr configuration 3				
B_5-Gr				
B_6-Gr				

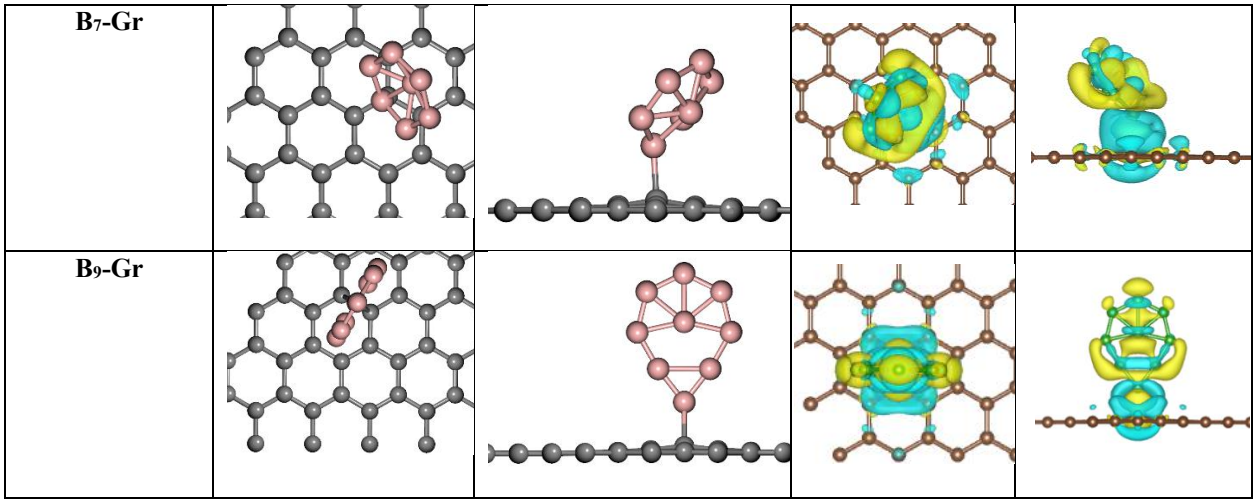


Fig. 2. Top and side view of B-Gr structures and top and side view of electron density difference (CDD) maps.

To understand a relationship between bond behavior and stability, COHP calculation is used as seen the parameters on Table 3. More negative values show more covalent bond behavior. Any bond has not ionic character because the value of ICHOP of bonds is not close to zero. The C-C bond in pristine graphene is -9.87 eV. After doping boron cluster, the strengths of C-C bond near the interaction is weakened in all structure while the C-C bonds far way from interaction in the honey cone become more covalent. The C-C bond has a higher value than the B-B bond, indicating stronger covalent behavior on the C-C bond. Inspection of the C-C values, they show similar values across all structures. This indicates that graphene lattice remains largely preserved after the interaction and still conserves its structure. The B-B bond in **B_3-Gr** (configuration 1) has more negative value (-7.43eV) because the interaction with the graphene is too low and the bonds are strongly connected to each other with covalent bond. Compared to other configuration of **B_3-Gr**, the ICHOP value on the B-B bond (~ -4.02eV) decreases because the bonds interact with the surface and the bond structures weaken. However, the B-B bond away from the graphene still maintains its high value. In structures with more negative Bader charge (e.g., **B_3-Gr configuration 3,** Δq=−0.98), there is more charge transfer between B-C atoms and the bond character between these atoms becomes stronger (more covalent character), which contributes to a more negative ICOHP. Since the ICHOP calculation at B9-Gr surface does not converge, the result is not written in Table 3.

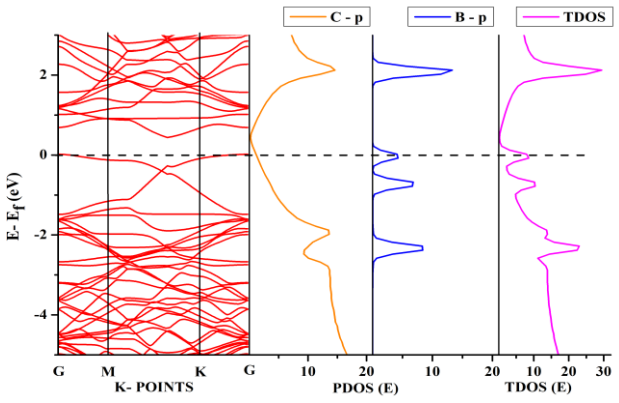
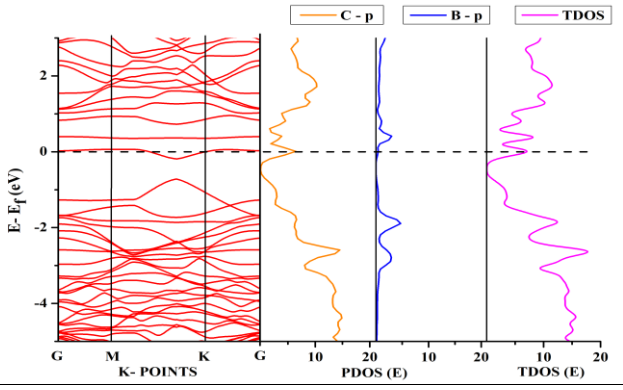
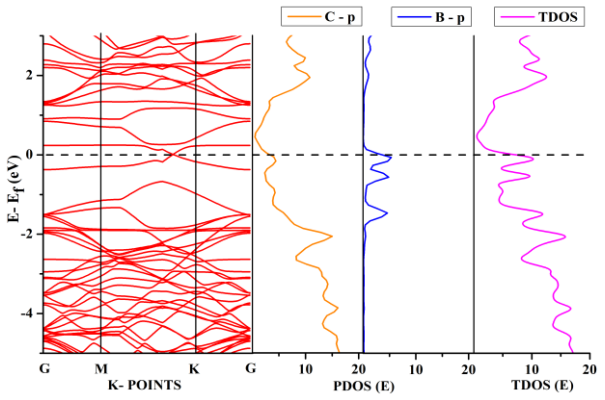
If Bader charge transferred is compared, **B_3** only gains charge in **the B_3-Gr configuration 1**, while boron clusters lost charge in all other structures. In **B_3-Gr configuration 1** in Fig. 2, the CDD maps show more clearly with the yellow zone (where the charge accumulates). There is no connection on the charges density between **B_3** cluster and graphene because of the weak interaction, and the distance between the boron cluster and the graphene (3.53 Å) is quite large. **B_3-Grconfiguration 2** and **3** have the higher Bader charge transfer than other structures have so their CDD maps exhibit more intensive charge transfer. The more intense yellow regions in **B_6-Gr** and **B_5-Gr** affect the electronic properties of the structure and also ensure that the structures are more stable. These results are reported for the first time in this study and therefore could not be compared with any previous research.

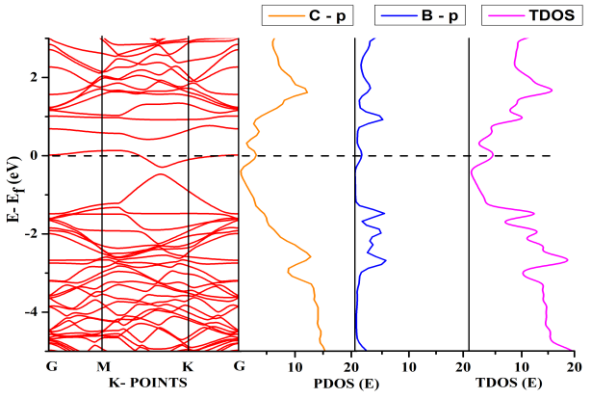
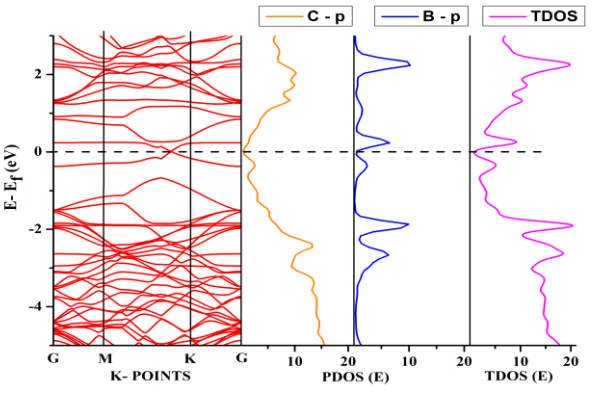
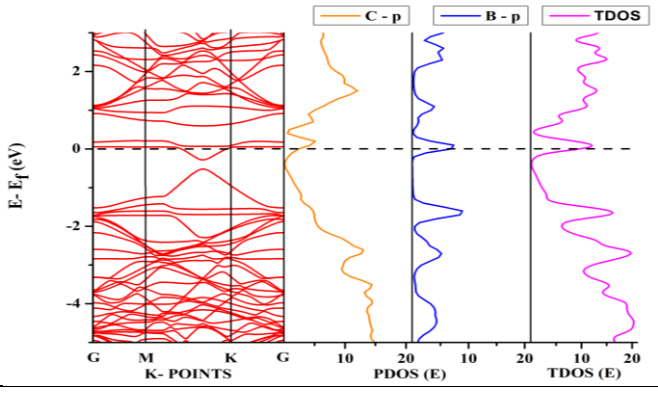
Table 3. Average values of ICOHP of bonds.

Structure	Bond	ICOHP (eV)
Pristine graphene	C-C	-9.87
	B-B	-7.43

B_3-Gr Configuration 1	C-C	-10.02
	B-B	-4.02, -7.85
B_3-Gr configuration 2	C-C	-8.45, -10.70
	B-C	-6.00
	B-B	-3.92, -7.75
B_3-Gr Configuration 3	C-C	-8.83, -10.20
	B-C	-5.94
	B-B	-6.20, -7.33
B_5-Gr	C-C	-8.91, -9.49
	B-C	-4.70
	B-B	-5.22, -7.11
B_6-Gr	C-C	-8.70, -10.30
	B-C	-4.67
	B-B	-3.76, -6.52,
B_7-Gr	C-C	-9.38
	B-C	-4.40

The band structure calculations and electron state density of materials are given in Fig. 3. Band gap values are in Table 2.Band structure determines the properties of a material such as conductor and insulator. The characteristic feature of two-dimensional pristine graphene in the band structure has the Dirac cone [45]. A similar intersection between K-M points is seen only in **B_3-Gr configuration 2** and **B_6-Gr** with a narrower cone structure. This shows that they are zero-gap semimetals with similar properties to pristine graphene. Cluster configuration and size significantly alter the band structure of graphene. This modification is critical for electronic applications because doping is required to overcome graphene's zero band gap problem. In **B_3-Gr configuration 1**, the Dirac cone has shifted below the Fermi energy. **B_3-Gr configuration 1, B_3-Gr configuration 3, B_5-Gr, B_7-Gr** and **B_9-Gr** structure have semiconductor properties. The density of state graph to the right of the band structures shows the energy levels of the p orbitals of the carbon and boron atoms and the total electron state density. In general, the contribution of the p orbital of the carbon atom to the total density is greater. The contribution of the p orbital of the B atom at near fermi levet prevents the structures from shifting to the insulating property. The band structure and DOS analyses confirm that boron cluster doping effectively tunes the electronic properties of graphene.

Structure	*Band and DOS*
B_3-Gr configuration 1	
B_3-Gr configuration 2	
B_3-Gr configuration 3	

B_5-Gr	
B_6-Gr	
B_7-Gr	

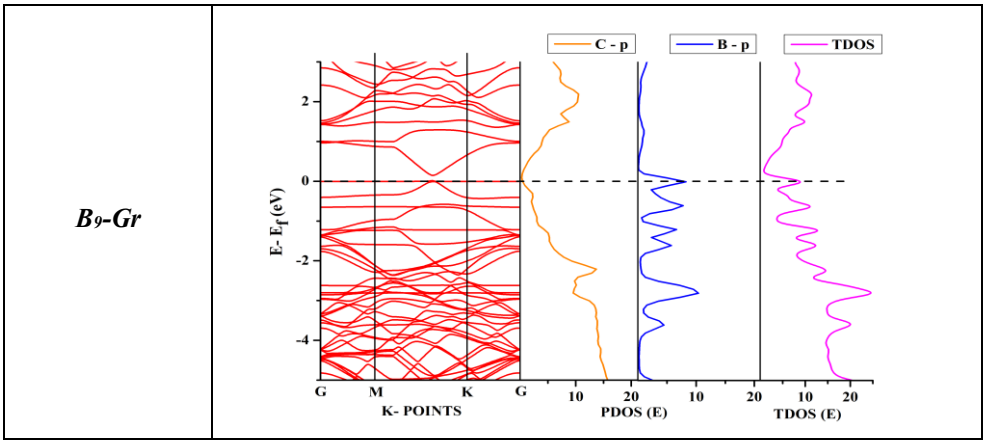


Fig. 3. Band structure (left) and electron density of state (DOS) graphs of B-Gr structures (right). The gamma point is denoted by G. C-p is the p orbital of carbon, B-p is the p orbital of boron atom, and TDOS is the total electron state density.

4. Conclusion

In this study, the electronic properties of graphene doped with B_3–B_9 boron clusters were theoretically investigated with DFT calculation. The results show that different interactions develop between graphene and boron clusters depending on the cluster size and configuration on the surface. In general, the weaker π–B interaction causes the cluster to adopt a vertical geometry to maximize B–C bonding and is observed to bond with only one boron atom. Among these structures, only graphene in the **B_3-Gr** cluster is able to stand parallel to the surface. However, the stability of this structure is quite low compared to other structures. These findings suggest that the size and orientation of the boron clusters are key factors in controlling the transition between semi-metallic and semiconducting behaviour. B_5-Gr and B_6-Gr exhibit the lowest formation energies, indicating their potential relevance for nanoelectronic applications. This study contributes to the understanding of boron-cluster functionalization in two-dimensional lightweight materials. Boron cluster-doped surfaces can be a good alternative for the search for both light and semiconductor material groups.

Acknowledgments

The numerical calculations reported in this paper were fully/partially performed at TUBITAK ULAKBIM, High Performance and Grid Computing Centre (TRUBA resources).

Author Contributions

Hilal Küçük: conceptualization, resources, methodology, investigation, project administration, writing-original draft and writing-review & editing.

İsa Baruğ: conceptualization, resources, investigation, project administration, writing-original draft and writing-review & editing.

Meryem Yurt: conceptualization, resources, investigation, project administration, writing-original draft and writing-review & editing.

References

[1] P. Ho, "Twenty years of 2D materials," *Nat. Phys,* vol. 20, no. 1,pp. 1, 2024.

[2] A. Rahman *et al.*, "Emerging 2D borophene: Synthesis, characterization, and sensing applications," *Sensors and Actuators A: Physical,* vol. 359,pp. 114468, 2023.

[3] V. D. Punetha, G. Nath, S. Pillai, and G. T. P. Azar, "Two-Dimensional Germanene Synthesis, Functionalization, and Applications," in *2D Materials: Chemistry and Applications (Part 2)*: Bentham Science Publishers, 2024, pp. 164-186.

[4] A. Mubeen and A. Majid, "Density Functional Theory Study on Magnetic character and Mn Crystal Field Split Levels in Mn-doped SnO Monolayer," *Journal of Superconductivity and Novel Magnetism,* vol. 35, no. 10, pp. 2975-2986, 2022/10/01 2022.

[5] E. P. Randviir, D. A. Brownson, and C. E. Banks, "A decade of graphene research: production, applications and outlook," *Materials Today,* vol. 17, no. 9, pp. 426-432, 2014.

[6] S. S. A. Kumar, S. Bashir, K. Ramesh, and S. Ramesh, "New perspectives on graphene/graphene oxide based polymer nanocomposites for corrosion applications: the relevance of the graphene/polymer barrier coatings," *Progress in Organic Coatings,* vol. 154,pp. 106215, 2021.

[7] C. Phillips, A. Al-Ahmadi, S.-J. Potts, T. Claypole, and D. Deganello, "The effect of graphite and carbon black ratios on conductive ink performance," *Journal of materials science,* vol. 52, no. 16, pp. 9520-9530, 2017.

[8] Y. J. Yun, W. G. Hong, W.-J. Kim, Y. Jun, and B. H. Kim, "A novel method for applying reduced graphene oxide directly to electronic textiles from yarns to fabrics," *Advanced Materials (Deerfield Beach, Fla.),* vol. 25, no. 40, pp. 5701-5705, 2013.

[9] E. W. Hill, A. Vijayaragahvan, and K. Novoselov, "Graphene sensors," *IEEE Sensors Journal,* vol. 11, no. 12, pp. 3161-3170, 2011.

[10] Y. Liu, X. Dong, and P. Chen, "Biological and chemical sensors based on graphene materials," *Chemical Society Reviews,* vol. 41, no. 6, pp. 2283-2307, 2012.

[11] A. E. Genç and I. Tranca, "Adsorption mechanism of the N 2 and NRR intermediates on oxygen modified MnN 4–graphene layers–a single atom catalysis perspective," *Physical Chemistry Chemical Physics,* vol. 25, no. 27, pp. 18465-18480, 2023.

[12] J. Li, H. Zheng, L. Liu, F. Meng, Y. Cui, and F. Wang, "Modification of graphene and graphene oxide and their applications in anticorrosive coatings," *Journal of Coatings Technology and Research,* vol. 18, pp. 311-331, 2021.

[13] Y. Tong, S. Bohm, and M. Song, "Graphene based materials and their composites as coatings," *Austin Journal of Nanomedicine & Nanotechnology,* vol. 1, no. 1, pp. 1003-1019, 2013.

[14] X. Cai, L. Lai, Z. Shen, and J. Lin, "Graphene and graphene-based composites as Li-ion battery electrode materials and their application in full cells," *Journal of Materials Chemistry A,* vol. 5, no. 30, pp. 15423-15446, 2017.

[15] B. Xu *et al.*, "What is the choice for supercapacitors: graphene or graphene oxide?," *Energy & Environmental Science,* vol. 4, no. 8, pp. 2826-2830, 2011.

[16] F. Schwierz, "Graphene transistors," *Nature nanotechnology,* vol. 5, no. 7, pp. 487-496, 2010.

[17] A. E. Genç, A. Akça, C. Karaman, M. B. Camarada, and E.-N. Dragoi, "Ammonia free catalytic reduction of nitric oxide on Ni-embedded graphene nanostructure: A density functional theory investigation," *Molecular Catalysis,* vol. 541,pp. 113119, 2023/04/15/ 2023.

[18] H. Küçük and A. Genç, "The effect of the chemical bonding environment changes in FeNX: Hydrocarbon adsorption by DFT," *Inorganic Chemistry Communications,pp.* 112165, 2024.

[19] D. Özkan, M. C. Özekinci, Z. T. Öztürk, and E. Sulukan, "Two Dimensional Materials for Military Applications," *Defence Science Journal,* vol. 70, no. 6, 2020.

[20] A. Mubeen and A. Majid, "First principles investigation of 3d transition metal doped SnO monolayer based diluted magnetic semiconductors," *Journal of Magnetism and Magnetic Materials,* vol. 580,pp. 170897, 2023/08/15/ 2023.

[21] A. Mubeen, A. Majid, S. Haider, and K. Alam, "Quantum electronic transport properties of 3d transition metal doped SnO monolayer for spin-thin film transistor," *Optical and Quantum Electronics,* vol. 56, no. 7,pp. 1169, 2024/06/08 2024.

[22] X. Cao, X. F. Li, and W. Hu, "Tunable Electronic and Magnetic Properties of Graphene-Embedded Transition Metal-N4 Complexes: Insight From First-Principles Calculations," *Chemistry–An Asian Journal,* vol. 13, no. 21, pp. 3239-3245, 2018.

[23] C. Jin *et al.*, "Adsorption of transition-metal clusters on graphene and N-doped graphene: a DFT study," *Langmuir,* vol. 38, no. 12, pp. 3694-3710, 2022.

[24] P. Rani and V. Jindal, "Designing band gap of graphene by B and N dopant atoms," *RSC advances,* vol. 3, no. 3, pp. 802-812, 2013.

[25] W. Wang, C. Zhao, and P. Li, "Tuning the electronic properties of graphene oxide nanoribbons through different oxygen doping configurations," *Journal of Electronic Materials,* vol. 47, no. 12, pp. 7093-7098, 2018.

[26] X. g. Luan *et al.*, "Design, preparation, and properties of a boron nitride coating of silica optical fiber for high temperature sensing applications," *Journal of Alloys and Compounds,* vol. 850,pp. 156782, 2021.

[27] X. Zhang *et al.*, "Synergistic boron doping of semiconductor and dielectric layers for high-performance metal oxide transistors: interplay of experiment and theory," *Journal of the American Chemical Society,* vol. 140, no. 39, pp. 12501-12510, 2018.

[28] C. Zhao, B. Xu, Z. Wang, and Z. Wang, "Boron-doped III–V semiconductors for Si-based optoelectronic devices," *Journal of Semiconductors,* vol. 41, no. 1,pp. 011301, 2020.

[29] L. Ma *et al.*, "Boron-based high-performance lithium batteries: Recent progress, challenges, and perspectives," *Advanced Energy Materials,* vol. 13, no. 25,pp. 2300042, 2023.

[30] E. H. Ezechi, M. H. Isa, S. R. Kutty, and N. B. Sapari, "Boron recovery, application and economic significance: A review," in *2011 National Postgraduate Conference*, 2011: IEEE, pp. 1-6.

[31] G. Bhimanapati, N. Glavin, and J. A. Robinson, "2D boron nitride: synthesis and applications," in *Semiconductors and semimetals*, vol. 95: Elsevier, 2016, pp. 101-147.

[32] N. Ay, G. M. Ay, and Y. Göncü, "Environmentally friendly material: Hexagonal boron nitride," *Journal of BORON,* vol. 1, no. 2, pp. 66-73, 2016.
[33] W.-L. Li, X. Chen, T. Jian, T.-T. Chen, J. Li, and L.-S. Wang, "From planar boron clusters to borophenes and metalloborophenes," *Nature Reviews Chemistry,* vol. 1, no. 10,pp. 0071, 2017.
[34] D. Kang *et al.*, "Probing the structure and electronic properties of beryllium doped boron clusters: A planar BeB16− cluster motif for metallo-borophene," *Scientific reports,* vol. 9, no. 1,pp. 14367, 2019.
[35] A. Kochaev, K. Katin, M. Maslov, and S. Singh, "Covalent and van der Waals interactions in a vertical heterostructure composed of boron and carbon," *Physical Review B,* vol. 105, no. 23,pp. 235444, 2022.
[36] J. Moellmann and S. Grimme, "DFT-D3 study of some molecular crystals," *The Journal of Physical Chemistry C,* vol. 118, no. 14, pp. 7615-7621, 2014.
[37] G. Kresse and D. Joubert, "From ultrasoft pseudopotentials to the projector augmented-wave method," *Physical review b,* vol. 59, no. 3,pp. 1758, 1999.
[38] J. P. Perdew, K. Burke, and M. Ernzerhof, "Generalized gradient approximation made simple," *Physical review letters,* vol. 77, no. 18,pp. 3865, 1996.
[39] B. Hammer, L. B. Hansen, and J. K. Nørskov, "Improved adsorption energetics within density-functional theory using revised Perdew-Burke-Ernzerhof functionals," *Physical review B,* vol. 59, no. 11,pp. 7413, 1999.
[40] R. A. van Santen and I. Tranca, "How molecular is the chemisorptive bond?," *Physical Chemistry Chemical Physics,* 10.1039/C6CP01394E vol. 18, no. 31, pp. 20868-20894, 2016.
[41] R. Y. Rohling, I. C. Tranca, E. J. M. Hensen, and E. A. Pidko, "Correlations between Density-Based Bond Orders and Orbital-Based Bond Energies for Chemical Bonding Analysis," *The Journal of Physical Chemistry C,* vol. 123, no. 5, pp. 2843-2854, 2019/02/07 2019.
[42] R. Dronskowski and P. E. Bloechl, "Crystal orbital Hamilton populations (COHP): energy-resolved visualization of chemical bonding in solids based on density-functional calculations," *The Journal of Physical Chemistry,* vol. 97, no. 33, pp. 8617-8624, 1993/08/01 1993.
[43] W. Tang, E. Sanville, and G. Henkelman, "A grid-based Bader analysis algorithm without lattice bias," *Journal of Physics: Condensed Matter,* vol. 21, no. 8,pp. 084204, 2009.
[44] I. Boustani, "Systematic ab initio investigation of bare boron clusters: mDetermination of the geometryand electronic structures of B n (n= 2–14)," *Physical Review B,* vol. 55, no. 24,pp. 16426, 1997.
[45] D. Malko, C. Neiss, F. Vines, and A. Görling, "Competition for graphene: graphynes with direction-dependent dirac cones," *Physical review letters,* vol. 108, no. 8,pp. 086804, 2012.